Eur. Phys. J. B **5**, 687–695 (1998)

THE EUROPEAN PHYSICAL JOURNAL B

Mixed spin transverse Ising model with longitudinal random crystal field interactions*

N. Benayad[1], R. Zerhouni[1], and A. Klümper[2,a]

[1] Groupe de Mécanique Statistique des Transitions de Phases et Phénomènes Critiques, Laboratoire de Physique Théorique, Université Hassan II, Faculté des Sciences Aîn Chock, BP 5366 Maârif, Casablanca, Morocco
[2] Institut für Theoretische Physik, Universität zu Köln, Zülpicher Strasse 77, 50937 Köln, Germany

Received: 13 February 1998 / Accepted: 17 March 1998

Abstract. The effect of a longitudinal random crystal field interaction on the phase diagrams of the mixed spin transverse Ising model consisting of spin-1/2 and spin-1 is investigated within the finite cluster approximation based on a single-site cluster theory. In order to expand a cluster identity of spin-1, we transform the spin-1 to spin-1/2 representation containing Pauli operators. We derive the state equations applicable to structures with arbitrary coordination number N. The phase diagrams obtained in the case of a honeycomb lattice ($N = 3$) and a simple-cubic lattice ($N = 6$), are qualitatively different and examined in detail. We find that both systems exhibit a variety of interesting features resulting from the fluctuation of the crystal field interactions.

PACS. 05.30.-d Quantum statistical mechanics – 05.50.+q Lattice theory and statistics; Ising problems – 05.70.-a Thermodynamics

1 Introduction

Over recent years there has been considerable interest in the theoretical study of transverse Ising models. The spin-1/2 transverse Ising model was originally introduced by de Gennes [1] as a valuable model for the tunneling of the proton in hydrogen-bonded ferroelectrics [2] such as the KH_2PO_4 type. Since then, it has been successfully applied to several physical systems, such as cooperative Jahn-teller systems [3] (like D_yVO_4, and $TbVO_4$), ordering in rare earth compounds with a singlet crystal-field ground state [4], and also to some real magnetic materials with strong uniaxial anisotropy in a transverse field [5]. It has been extensively studied by the use of various techniques [6–9], including the effective field theory [10,11] based on a generalized but approximated Callen-Suzuki relation derived by Sà Barreto, Fittipaldi and Zeks. In addition to the works on the two-state spin systems, the spin-one transverse Ising models [12–14] have received some attention. The influence of the crystal field interaction on its phase diagram has also been investigated [15].

Recently, attention has been directed to the study of the magnetic properties of a two-sublattice mixed spin Ising systems. They are of interest for the following main reasons. They have less translational symmetry than their single spin counterparts, and are well adapted to study a certain type of ferrimagnetism [16]. It has been shown that the MnNi(EDTA)-$6H_2O$ complex is an example of a mixed spin system [17]. The mixed Ising spin system consisting of spin-1/2 and spin-1 has been studied by renormalization group technique [18,19], by high-temperature series expansions [20], by free-fermion approximation [21] and by finite cluster approximation [22]. The effects of single ion anisotropy on its transition temperature have been investigated by the renormalization group method [19], Monte-Carlo simulation in the case of a square lattice [23], effective field theory with correlations [24] and finite cluster approximation [25]. The two latter methods predict a tricritical behaviour in systems with a coordination number N larger than three. It is important to note here that the exact solution for the transition temperature, which is always of second order, can be obtained analytically if the structure of the system is chosen to be a honeycomb lattice ($N = 3$) [26,27].

Very recently, we have investigated [28], using the finite cluster approximation [29,30], the influence of a transverse field on the magnetic properties of the three dimensional ($N = 6$) mixed spin-1/2 and spin-1 Ising system with uniform longitudinal crystal field interactions. We have found that the system keeps a tricritical behaviour only when the transverse field strength is relatively small; otherwise the critical behaviour disappears and all transitions are always of second order for any values of the crystal field interaction and the transverse field. In this latter study, we have neglected the fluctuations of the crystal field interaction.

* Dedicated to J. Zittartz on the occasion of his 60th birthday

[a] e-mail: kluemper@thp.uni-koeln.de

The purpose of this paper is to examine the effects of the fluctuations of a longitudinal crystal field interaction on the phase diagram of the mixed spin-1/2 and spin-1 transverse Ising system. Such a system may be described by the following Hamiltonian

$$H=-\sum_{\langle ij\rangle} J_{ij}\sigma_{iz}S_{jz}-\Omega_1\sum_i \sigma_{ix}-\Omega_2\sum_j S_{jx}+\sum_j D_j S_{jz}^2 \tag{1}$$

where $\sigma_{i\alpha}$ and $S_{j\alpha}(\alpha = x, z)$ are the α-components of spin-1/2 and spin-1 operators at sites i and j, respectively. $J_{ij} = J$ is the exchange interaction and the first summation is carried out only over nearest-neighbour pairs of spins. Ω_1 and Ω_2 are the transverse fields, and D_j is assumed to be randomly distributed according to an independent probability distribution function $P(D_j)$,

$$P(D_j)=\frac{1}{2}\{\delta\left[D_j-D(1+d)\right]+\delta\left[D_j-D(1-d)\right]\} \tag{2}$$

with

$$d=\frac{\Delta D}{D}\leq 1, \tag{3}$$

where ΔD is the fluctuation from the mean value D.

To this end, we use the finite cluster approximation [29,30] with an expansion technique for cluster identities of spin-1 localized on one sublattice, which correctly accounts for the single-site kinematic relations.

Our presentation is as follows. In Section 2 we describe the theoretical framework and calculate the state equations. In Section 3 we investigate and discuss the phase diagrams for the honeycomb lattice ($N = 3$) and the simple cubic lattice ($N = 6$).

2 Finite cluster approximation

The theoretical framework to be used in the study of the system described by the Hamiltonian (1) is the Finite Cluster Approximation (FCA), based on a single-site cluster theory. In this method, attention is focused on a cluster comprising just a single selected spin $\sigma_o(S_o)$, and its nearest-neighbour spins $\{S_1, S_2, ..., S_N\}$ ($\{\sigma_1, \sigma_2, ..., \sigma_N\}$), with which it directly interacts. We split the total Hamiltonian (1) into two parts, $H = H_o + H'$, where H_o includes all parts of H associated with the lattice site o. In the present system, H_o takes the form

$$H_{o\sigma}=A_1\sigma_{oz}+B_1\sigma_{ox}, \tag{4}$$

$$H_{oS}=A_2S_{oz}+B_2S_{ox}+D_oS_{oz}^2, \tag{5}$$

where

$$A_1=-J\sum_{j=1}^{N}S_{jz},\ B_1=-\Omega_1,\ A_2=-J\sum_{i=1}^{N}\sigma_{iz},\ B_2=-\Omega_2, \tag{6}$$

if the lattice site o belongs to σ- or S-sublattice, respectively.

The problem consists in evaluating the sublattice longitudinal and transverse components of the magnetization and the quadrupolar moments. In order to calculate them, we choose a representation in which σ_{oz} and S_{oz} are diagonal and denote by $\langle\sigma_{o\alpha}\rangle_c$ and $\langle S_{o\alpha}^n\rangle_c^\varepsilon$, ($\varepsilon = +$ or $-$ and $n = 1, 2$), respectively, the mean value of $\sigma_{o\alpha}$ and $S_{o\alpha}$ for a given configuration c of all other spins (*i.e.* when all other spin σ_i and S_j ($i, j \neq 0$) have fixed values) and a fixed configuration $\{D_i = (1\pm d)D\}$ of the random crystal field. Neglecting the fact that H_o and H' do not commute, $\langle\sigma_{o\alpha}\rangle_c$ and $\langle S_{o\alpha}^n\rangle_c^\varepsilon$, are given by

$$\langle\sigma_{o\alpha}\rangle_c=\frac{Tr_{\sigma_o}\sigma_{o\alpha}\exp(-\beta H_{o\sigma})}{Tr_{\sigma_o}\exp(-\beta H_{o\sigma})} \tag{7}$$

$$\langle S_{o\alpha}^m\rangle_c^\varepsilon=\frac{Tr_{S_o}S_{o\alpha}^n\exp(-\beta H_{oS})}{Tr_{S_o}\exp(-\beta H_{oS})} \tag{8}$$

where $Tr_{\sigma o}$ (or Tr_{So}) means the trace performed over σ_o (or S_o) only. As usual $\beta = 1/T$, where T is the absolute temperature. Since the crystal field D_i on the site i is assumed to take on two values $D(1 \pm d)$ with equal probability, the sublattice magnetizations μ_α, m_α and the quadrupolar moments $q_\alpha(\alpha = x, z)$ are then given by

$$\mu_\alpha\equiv\left\langle\langle\sigma_{o\alpha}\rangle_c\right\rangle=\left\langle\frac{Tr_{\sigma_o}\sigma_{o\alpha}\exp(-\beta H_{o\sigma})}{Tr_{\sigma_o}\exp(-\beta H_{o\sigma})}\right\rangle, \tag{9}$$

$$\begin{aligned} m_\alpha &\equiv \frac{1}{2}\left\langle\langle S_{o\alpha}\rangle_c^+ + \langle S_{o\alpha}\rangle_c^-\right\rangle \\ &= \frac{1}{2}\left\langle\left.\frac{Tr_{S_o}S_{o\alpha}\exp(-\beta H_{oS})}{Tr_{S_o}\exp(-\beta H_{oS})}\right|_{D_o=D(1+d)}\right. \\ &\quad \left.+\left.\frac{Tr_{S_o}S_{o\alpha}\exp(-\beta H_{oS})}{Tr_{S_o}\exp(-\beta H_{oS})}\right|_{D_o=D(1-d)}\right\rangle, \end{aligned} \tag{10}$$

$$\begin{aligned} q_\alpha &\equiv \frac{1}{2}\left\langle\langle S_{o\alpha}^2\rangle_c^+ + \langle S_{o\alpha}^2\rangle_c^-\right\rangle \\ &= \frac{1}{2}\left\langle\left.\frac{Tr_{S_o}S_{o\alpha}^2\exp(-\beta H_{oS})}{Tr_{S_o}\exp(-\beta H_{oS})}\right|_{D_o=D(1+d)}\right. \\ &\quad \left.+\left.\frac{Tr_{S_o}S_{o\alpha}^2\exp(-\beta H_{oS})}{Tr_{S_o}\exp(-\beta H_{oS})}\right|_{D_o=D(1-d)}\right\rangle, \end{aligned} \tag{11}$$

which can be considered as the starting point of the single-site cluster approximation. $\langle ...\rangle$ denotes the average over all spin configurations. Equations (9) to (11) are not exact. Neverthless, they have been accepted as a reasonable starting point [10] for transverse Ising systems and have been successfully applied to a number of interesting transverse Ising models [10,11,28]. We have to emphasize that in the Ising limit ($\Omega_1 = \Omega_2 = 0$), the Hamiltonian (1) contains only σ_{iz} and S_{jz}. Then, the relations (9, 10, 11) become exact identities.

To calculate $\langle\sigma_{o\alpha}\rangle_c$ and $\langle S_{o\alpha}^n\rangle_c^\varepsilon$ one has first to diagonalize the single-site Hamiltonians $H_{o\sigma}$ and H_{os}, respectively. $H_{o\sigma}$ can be written in a diagonal form if we use the

following rotation transformation

$$\sigma_{oz} = \cos\varphi\sigma_{oz'} - \sin\varphi\sigma_{ox'} \tag{12}$$

$$\sigma_{ox} = \sin\varphi\sigma_{oz'} + \cos\varphi\sigma_{ox'}, \tag{13}$$

with

$$\cos\varphi = \frac{-A_1}{\left[A_1^2+B_1^2\right]^{1/2}},\ \sin\varphi = \frac{-B_1}{\left[A_1^2+B_1^2\right]^{1/2}}\cdot \tag{14}$$

Then, evaluating the inner traces in (7) over the states of the selected spin σ_o, we obtain

$$\langle\sigma_{oz}\rangle_c = \frac{-A_1}{2\left[A_1^2+B_1^2\right]^{1/2}}\tanh\left\{\frac{\beta}{2}\left[A_1^2+B_1^2\right]^{1/2}\right\} \tag{15}$$

$$\langle\sigma_{ox}\rangle_c = \frac{-B_1}{2\left[A_1^2+B_1^2\right]^{1/2}}\tanh\left\{\frac{\beta}{2}\left[A_1^2+B_1^2\right]^{1/2}\right\}\cdot \tag{16}$$

H_{os} can also readily be diagonalized. Its eigenvalues γ_k are given by

$$\gamma_k = \frac{2}{3}\left(D_o + \sqrt[3]{\eta}\cos(\theta_k)\right),\ k=1,2,3 \tag{17}$$

with

$$\theta_k = \frac{1}{3}\arccos\left(\frac{-27\,\overline{r}}{2\eta}\right) + \frac{2}{3}(k-1)\pi \tag{18}$$

$$\eta = \frac{3\sqrt{3}}{2}\left[27(\overline{r})^2 + \left|4r^3+27(\overline{r})^2\right|\right]^{1/2} \tag{19}$$

and

$$r = -(A_2^2+B_2^2) - \frac{D_o^2}{9},\ \overline{r} = -\frac{D_o}{3}\left(2A_2^2 - \frac{2}{9}D_o^2 - B_2^2\right)\cdot \tag{20}$$

The corresponding eigenvectors are

$$|\chi\rangle_k = a_k|+\rangle + b_k|-\rangle + c_k|o\rangle, \tag{21}$$

with

$$a_k = \frac{|B_2(\gamma_k - D_o + A_2)|}{\sqrt{2}\left\{B_2^2\left[(\gamma_k-D_o)^2+A_2^2\right] + \left[(\gamma_k-D_o)^2-A_2^2\right]^2\right\}^{1/2}} \tag{22}$$

$$b_k = \frac{\gamma_k - D_o - A_2}{\gamma_k - D_o + A_2}a_k,\ c_k = \frac{\sqrt{2}}{B_2}(\gamma_k - D_o - A_2)a_k. \tag{23}$$

Using the above eigenvalues and eigenvectors, to perform the inner traces in (8) over the states of the selected spin S_o and setting $n = 1$ and 2, we obtain

$$\langle S_{oz}\rangle_c^{\pm} = \frac{\sum_{k=1}^{3}\left[(a_k^{\pm})^2 - (b_k^{\pm})^2\right]\exp(-\beta\gamma_k^{\pm})}{\sum_{k=1}^{3}\exp(-\beta\gamma_k^{\pm})}, \tag{24}$$

$$\langle S_{ox}\rangle_c^{\pm} = \sqrt{2}\frac{\sum_{k=1}^{3}(a_k^{\pm}+b_k^{\pm})c_k^{\pm}\exp(-\beta\gamma_k^{\pm})}{\sum_{k=1}^{3}\exp(-\beta\gamma_k^{\pm})}, \tag{25}$$

$$\langle S_{oz}^2\rangle_c^{\pm} = \frac{\sum_{k=1}^{3}\left[(a_k^{\pm})^2 + (b_k^{\pm})^2\right]\exp(-\beta\gamma_k^{\pm})}{\sum_{k=1}^{3}\exp(-\beta\gamma_k^{\pm})}, \tag{26}$$

$$\langle S_{ox}^2\rangle_c^{\pm} = \frac{\sum_{k=1}^{3}\left[\frac{1}{2}(a_k^{\pm}+b_k^{\pm})^2 + (c_k^{\pm})^2\right]\exp(-\beta\gamma_k^{\pm})}{\sum_{k=1}^{3}\exp(-\beta\gamma_k^{\pm})}, \tag{27}$$

where

$$a_k^{\pm} = a_k(D_o = (1\pm d)D),\ b_k^{\pm} = b_k(D_o = (1\pm d)D),$$
$$c_k^{\pm} = c_k(D_o = (1\pm d)D),\ \gamma_k^{\pm} = \gamma_k(D_o = (1\pm d)D). \tag{28}$$

From equations (15, 16, 24−27), we easily observe that the sublattice magnetizations μ_α, m_α and quadrupolar moments q_α are functions of $\sum_j S_{jz}$ or $\sum_i \sigma_{iz}$. They can be written as

$$\mu_\alpha = \left\langle h_\alpha\left(\sum_{j=1}^{N} S_{jz}\right)\right\rangle,$$
$$m_\alpha = \left\langle f_\alpha\left(\sum_{i=1}^{N}\sigma_{iz}\right)\right\rangle,$$
$$q_\alpha = \left\langle g_\alpha\left(\sum_{i=1}^{N}\sigma_{iz}\right)\right\rangle, \tag{29}$$

with

$$h_\alpha\left(\sum_{j=1}^{N} S_{jz}\right) = \langle\sigma_{o\alpha}\rangle_c, \tag{30}$$

$$f_\alpha\left(\sum_{i=1}^{N}\sigma_{iz}\right) = \frac{1}{2}\left[\langle S_{o\alpha}\rangle_c^{+} + \langle S_{o\alpha}\rangle_c^{-}\right], \tag{31}$$

$$g_\alpha\left(\sum_{i=1}^{N}\sigma_{iz}\right) = \frac{1}{2}\left[\langle S_{o\alpha}^2\rangle_c^{+} + \langle S_{o\alpha}^2\rangle_c^{-}\right]. \tag{32}$$

When calculating the average on the right hand side of equations (29), we use the fact that any function $E(\sigma_z)$ and $\overline{E}(S_z)$ of $\sigma_z(=\pm 1/2)$ and $S_z(=0,\pm 1)$ can be written as the linear superposition

$$E(\sigma_z) = E_1 + E_2\sigma_z, \tag{33}$$

$$\overline{E}(S_z) = \overline{E}_1 + \overline{E}_2 S_z + \overline{E}_3 S_z^2, \tag{34}$$

with appropriate coefficients $E_{1,2}$ and $\overline{E}_{1,2,3}$. Applying this to all spins σ_{iz} and S_{jz} in equations (30−32), the functions h_α, f_α and g_α are decomposed as

$$h_\alpha\left(\sum_{j=1}^{N} S_{jz}\right) = \sum_{q=0}^{N}\sum_{p=0}^{N-q} H_{p,q}^{\alpha}\{S_z^2, S_z\}_{N,p,q}, \tag{35}$$

$$f_\alpha\left(\sum_{i=1}^{N}\sigma_{iz}\right) = \sum_{q=0}^{N} F_q^{\alpha}(N)\{\sigma_z\}_{N,q}, \tag{36}$$

$$g_\alpha\left(\sum_{i=1}^{N}\sigma_{iz}\right) = \sum_{q=0}^{N} G_q^{\alpha}(N)\{\sigma_z\}_{N,q}, \tag{37}$$

where $\{S_z^2, S_z\}_{N,p,q}$ denotes the superposition of all the terms containing p factors of S_{jz}^2 and q factors of $S_{j'z}$ with $j \neq j'$. These factors are selected from the

set $\{S_{1z}, S_{2z}, ..., S_{Nz}, S_{1z}^2, S_{2z}^2, ..., S_{Nz}^2\}$. For example, if $N = 4$, $p = 2$ and $q = 1$, then

$$\begin{aligned}\{S_z^2, S_z\}_{4,2,1} = S_{1z}(&S_{2z}^2S_{3z}^2 + S_{2z}^2S_{4z}^2 + S_{3z}^2S_{4z}^2)\\ &+ S_{2z}(S_{1z}^2S_{3z}^2 + S_{1z}^2S_{4z}^2 + S_{3z}^2S_{4z}^2)\\ &+ S_{3z}(S_{1z}^2S_{2z}^2 + S_{1z}^2S_{4z}^2 + S_{2z}^2S_{4z}^2)\\ &+ S_{4z}(S_{1z}^2S_{2z}^2 + S_{1z}^2S_{3z}^2 + S_{2z}^2S_{3z}^2). \quad (38)\end{aligned}$$

$\{\sigma_z\}_{N,q}$ denotes the superposition of all the terms containing q different factors of σ_{iz} selected from the set $\{\sigma_{1z}, \sigma_{2z}, ..., \sigma_{Nz}\}$. It may be noted that the coefficients $F_q^{(\alpha)}(N)$ and $G_q^{(\alpha)}(N)$ for spin-1/2 depend on the nearest-neighbours coordination number N, whereas the coefficients $H_{p,q}^{\alpha}$ are in fact independent of N.

Now, the problem is to determine the coefficients $H_{p,q}^{\alpha}$, $F_q^{(\alpha)}(N)$ and $G_q^{(\alpha)}(N)$. To evaluate $H_{p,q}^{\alpha}$, it is advantageous to transform the spin-1 system to spin-1/2 representation containing the Pauli operators $\overline{\sigma}_{jz} = \pm 1$ [31], by setting $S_{jz} = \tau_{jz}\overline{\sigma}_{jz}$ with $\tau_{jz} = 0, 1$. In this representation (35) becomes

$$h_\alpha\left(\sum_{j=1}^{N}\tau_{jz}\overline{\sigma}_{jz}\right) = \sum_{q=0}^{N}\sum_{p=0}^{N-q}H_{p,q}^{\alpha}\{\tau_z, \tau_z\overline{\sigma}_z\}_{N,p,q}, \quad (39)$$

which must be satisfied for arbitrary choices of τ_{jz}. Now let us choose the first r out of the N operators τ_{jz} to be unity, and the remainder zero. Then (39) gives

$$h_\alpha\left(\sum_{j=1}^{r}\overline{\sigma}_{jz}\right) = \sum_{q=0}^{r}\sum_{p=0}^{r-q}H_{p,q}^{\alpha}C_p^{r-q}\{\overline{\sigma}_z\}_{r,q}, \quad (40)$$

where $\{\overline{\sigma}_z\}_{r,q}$ has the same meaning as $\{\sigma_z\}_{N,q}$, but σ_{jz} and N are replaced by $\overline{\sigma}_{jz}$ and r, respectively. C_n^m are the binomial coefficients $m!/[n!(m-n)!]$. That is

$$h_\alpha\left(\sum_{j=1}^{r}\overline{\sigma}_{jz}\right) = \sum_{q=0}^{r}e_q^{(\alpha)}(r)\{\overline{\sigma}_z\}_{r,q}, \quad (41)$$

with

$$e_q^{(\alpha)}(r) = \sum_{p=0}^{r-q}H_{p,q}^{\alpha}C_p^{r-q}. \quad (42)$$

As is clear from equation (42), the coefficients $e_q^{(\alpha)}(r)$ for the spin-1/2 problem depend on the total number of the present spins. The above transformation of the spin-1 problem of (35) containing N spins to spin-1/2 problem containing r spins, enables us to use directly the results already established in [32] for the spin-1/2 system. Applying these results to the single group of r spins (41), we obtain

$$e_q^{(\alpha)}(r) = \frac{1}{2^rC_q^r}\sum_{n_1=0}^{r}C_{n_1}^r\varepsilon_{n_1}(r,q)h_{n_1\alpha}(r-2n_1), \quad (43)$$

where

$$\varepsilon_{n_1}(r,q) = \sum_{i=0}^{n_1}(-1)^iC_i^{n_1}C_{q-i}^{r-n_1}. \quad (44)$$

Once the coefficients $e_q^{(\alpha)}(r)$ have been calculated, the coefficients $H_{p,q}^{\alpha}$ may be found by the following procedure. First, $H_{o,q}^{(\alpha)}$ is obtained by setting $r = q$ in (42). That is

$$H_{o,q}^{(\alpha)} = e_q^{(\alpha)}(q). \quad (45)$$

By expressing (42) as a recurrence relation, namely,

$$H_{r-q,q}^{(\alpha)} = e_q^{(\alpha)}(r) - \sum_{p=0}^{r-q-1}H_{p,q}^{(\alpha)}C_p^{r-q}, \quad (46)$$

and using (43) we obtain the coefficients $H_{1,q}^{(\alpha)}$; $H_{2,q}^{(\alpha)}$; ...; $H_{N-q,q}^{(\alpha)}$ when $r = q+1$, $q+2$, ..., N, respectively. Thus, doing this for each value of $q\,(\in \{1, 2, ..., N\})$, we determine all the coefficients $H_{p,q}^{\alpha}$ appearing *via* the right-hand side of (35). On the other hand, to calculate $\langle f_\alpha(\sum_i \sigma_{iz})\rangle$ and $\langle g_\alpha(\sum_i \sigma_{iz})\rangle$ we use directly the results established in [32] for the spin-1/2 system. Then the coefficients $F_q^{(\alpha)}(N)$ and $G_q^{(\alpha)}(N)$ are given by

$$F_q^{(\alpha)}(N) = \frac{1}{2^{N-q}C_q^N}\sum_{n_2=0}^{N}C_{n_2}^N\varepsilon_{n_2}(N,q)f_{n_2\alpha}\left[\frac{1}{2}(N-2n_2)\right], \quad (47)$$

$$G_q^{(\alpha)}(N) = \frac{1}{2^{N-q}C_q^N}\sum_{n_3=0}^{N}C_{n_3}^N\varepsilon_{n_3}(N,q)g_{n_3\alpha}\left[\frac{1}{2}(N-2n_3)\right], \quad (48)$$

where

$$\varepsilon_n(N,q) = \sum_{i=0}^{n}(-1)^iC_i^nC_{q-i}^{N-n},\ n = n_2 \text{ or } n_3. \quad (49)$$

The sublattice magnetizations μ_α and m_α and the quadrupolar moments $q_\alpha(\alpha = z, x)$ are given by equations (29). They are valid for any lattice (arbitrary coordination number N), and constitute a set of relations, according to which we can study the present system. However, in order to carry out the average over all spin configurations implied in these equations, we have to deal with multispin correlations functions. The problem becomes mathematically untractable if we try to treat them in the spirit of the FCA. In this work, we use the simplest approximation in which the correlations between quantities pertaining to different sites are neglected,

$$\begin{aligned}\langle\sigma_{iz}\sigma_{kz}...\sigma_{lz}\rangle &\cong \langle\sigma_{iz}\rangle\langle\sigma_{kz}\rangle...\langle\sigma_{lz}\rangle\\ \langle S_{jz}^{p_1}S_{mz}^{p_2}...S_{nz}^{p_4}\rangle &\cong \langle S_{jz}^{p_1}\rangle\langle S_{mz}^{p_2}\rangle...\langle S_{nz}^{p_4}\rangle, \quad (50)\end{aligned}$$

with $i \neq k \neq ... \neq l$, $j \neq m \neq ... \neq n$, and $p_i = 1$ or 2. If this is done, and counting the number of elements

of the sets $\{S_z^2, S_z\}_{N,p,q}$ and $\{\sigma_z\}_{N,q}$ which are equal, respectively, to $C_p^N C_q^{N-p}$ and C_q^N, we find the following coupled equations

$$\mu_\alpha = \sum_{q=0}^{N} \sum_{p=0}^{N-q} C_p^N C_q^{N-p} H_{p,q}^{(\alpha)} m_z^q q_z^p, \tag{51}$$

$$m_\alpha = \sum_{q=0}^{N} C_q^N F_q^{(\alpha)}(N) \mu_z^q, \tag{52}$$

$$q_\alpha = \sum_{q=0}^{N} C_q^N G_q^{(\alpha)}(N) \mu_z^q. \tag{53}$$

3 Results and discussions

In this paper we are first interested in investigating the phase diagrams of the system in the case of a uniformly applied transverse field ($\Omega_1 = \Omega_2 = \Omega$) when the structure of the system is the honeycomb lattice ($N = 3$) and the simple cubic lattice ($N = 6$). At high temperature, the longitudinal magnetizations μ_z and m_z are zero. Below a transition temperature T_c, we have spontaneous ordering $\mu_z \neq 0$ and $m_z \neq 0$, while the corresponding transverse magnetizations μ_x and m_x are expected to be unequal zero at all temperatures. To calculate T_c, we substitute m_z and q_z in (51) with their expressions taken from (52) and (53). Then, we obtain an equation for μ_z of the form

$$\mu_z = a(T, D, \Omega, d)\mu_z + b(T, D, \Omega, d)\mu_z^3 + ..., \tag{54}$$

where

$$a = N^2 F_1^{(z)} \sum_{p=0}^{N-1} C_p^{N-1} H_{p,1}^{(z)} \left(G_0^{(z)}\right)^p, \tag{55}$$

and

$$\begin{aligned} b = N \sum_{p=0}^{N-1} C_p^{N-1} H_{p,1}^{(z)} \big[& NpC_2^N F_1^{(z)} G_2^{(z)} \left(G_0^{(z)}\right)^{p-1} \\ & + C_3^N F_3^{(z)} \left(G_0^{(z)}\right)^p \big] \\ + N^3 \sum_{p=0}^{N-3} & C_p^N C_3^{N-p} H_{p,3}^{(z)} \left(F_1^{(z)}\right)^3 \left(G_0^{(z)}\right)^p, \end{aligned} \tag{56}$$

within this approximation. As usual, the second-order transition temperature T_c, as a function of Ω, D and d, is then determined by the condition

$$a(T_c, \Omega, D, d) = 1. \tag{57}$$

The magnetization μ_z in the vicinity of the second-order transition is given by

$$\mu_z^2 = \frac{1-a}{b}\,. \tag{58}$$

The right-hand side of (58) must be positive. If this is not the case, the transition is of first-order, and the point at which

$$a = 1 \quad \text{and} \quad b = 0, \tag{59}$$

characterizes the tricritical point.

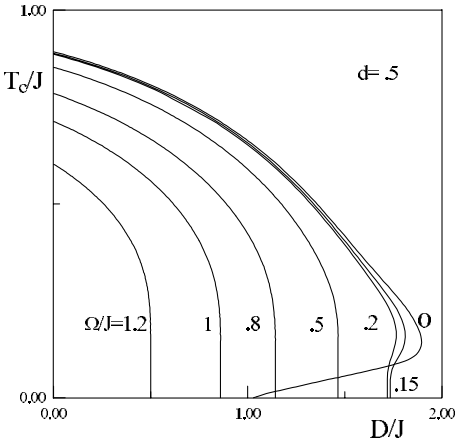

Fig. 1. The phase diagram in $T-D$ plane of the mixed spin-1/2 and spin-1 transverse Ising model on the honeycomb lattice ($N = 3$), when $d = 0.5$. The number accompanying each curve denotes the value of Ω/J.

3.1 The honeycomb lattice

Let us first investigate the phase diagram of the system when its structure is the honeycomb lattice ($N = 3$). This system does not exhibit a tricritical behaviour for any values of the parameters T, D, Ω and d. This means that the tricritical behaviour does not exist in the system with $N = 3$ even if the fluctuation of the crystal field interaction is taken into account.

In order to have an idea on the effects of a fluctuation of the crystal field on the mixed spin transverse Ising model, we have plotted in Figure 1 the phase diagrams in the (T, D) plane, for a fixed value of $d\,(d = 0.5)$ and selected values of the transverse field Ω. When $\Omega = 0$, the critical temperature T_c decreases with the increase of D, and at low temperatures a reentrant phenomenon appears. This effect is due to the competition between the exchange interaction and the fluctuation of the crystal field. We also plot in the figure, various transition lines when the strength of the transverse field takes values less than the critical one $\Omega_c\,(\Omega_c = 1.42$ J [28]). It is seen that the system exhibits a reentrant behaviour only when Ω is relatively small ($0 \leq \Omega \leq 0.48$ J) and disappears when Ω is larger than $\Omega = 0.48$ J. Thus, the fluctuation of the longitudinal crystal field has especially a qualitative influence on the mixed spin transverse Ising model only for not large values of the transverse field.

Reentrance in this sense can be explained by a competition of energy E and entropy S in the free energy $F = E - TS$. The entropy (measuring the disorder of the state) is usually less important at low temperatures. For pure systems the energy term becomes dominant and an ordered state of the physical system is preferred. However, for a magnetic system with random crystal field an effective reduction of the energy E as compared with a disordered state may not be possible for all interaction parameters. First of all, the crystal field D by itself energetically disfavours the state with $|S_j| = 1$ for positive

values of D. Secondly, the fluctuation d of the crystal field induces inherent disorder. For a given set of D and d this conspires to a thermodynamic state with $\langle S_j \rangle = 0$ for sufficiently low and sufficiently high temperature, but with $\langle S_j \rangle > 0$ for some intermediate temperature and hence $\langle \sigma_j \rangle > 0$. The transversal field is expected to order the system in transversal direction and to reduce the effect of disorder. This qualitative expectation is indeed verified by our quantitative calculations.

In Figure 2a, the variation of T_c with D is plotted in the absence of the transverse field ($\Omega = 0$) and for various values of d. When the fluctuations of the crystal field are neglected ($d = 0$), the critical temperature decreases gradually with D and vanishes at the exact critical value $D_c = 1.5$ J of the crystal field. Such behaviour is predicted by the exact calculation [26,27]. But, for finite d, the reentrant phenomenon appears and it becomes more and more pronounced with increasing values of d. We also note that for small D, T_c does not depend on the value of d, as seen in Figure 2a. From this property and due to the fluctuations of the crystal field, the phase boundary lines can take a finite value even for the value of D larger than D_c. We note that in a small transverse field Ω ($0 \leq \Omega \leq 0.48$ J), the system keeps this behaviour for any value of d. But for Ω larger than $\Omega = 0.48$ J, the above reentrant behaviour completely disappears. In this case, when Ω belongs to the restricted region $0.48 < \Omega/J < 0.94$, for high transition temperatures T_c, the system is not sensitive to the fluctuation of the crystal field, while at low T_c, it remarkably depends on the value of d, as is clearly shown in Figure 2b for $\Omega = 0.5$ J. One important result is exhibited by the system when Ω approaches ($0.94 \leq \Omega/\mathrm{J} < \Omega_c$) its critical value $\Omega_c = 1.42$ J. In fact, in this range, the ferromagnetic frontier is independent of the fluctuation of the crystal field as seen in Figure 2c for $\Omega = 1.0$ J.

In order to clarify the influence of d on the transition temperature T_c in the mixed spin transverse Ising model on the honeycomb lattice, we study the changes of T_c with d for fixed D and selected values of the transverse field. In this case, low and high values of the mean value D of the crystal field lead to two different behaviours of T_c with d: i) as is depicted in Figure 3a ($D/\mathrm{J} = 1$), for low D, the critical temperature expresses a small variation with the increase of d for any strength of the transverse field Ω less than Ω_c; ii) as is plotted in Figure 3b, ($D = 1.5$ J), for relatively high D, the phase diagram exhibits in $T - d$ plane a reentrant phenomenon for small values of the transverse field Ω. In general the ferromagnetic phase increases with increasing d. This can be explained by clusters in the system with small crystal field, therefore these clusters order at higher temperatures. The transversal field reduces the longitudinal ferromagnetic order except at very low temperature where the transversal field is acting against the disorder. At low T and small transversal fields the reentrance phenomenon is reduced. Hence, there appears magnetic order in spin space with transversal as well as longitudinal components! This can be seen in Figure 3b. Note that the bulge in the phase boundary (reentrant

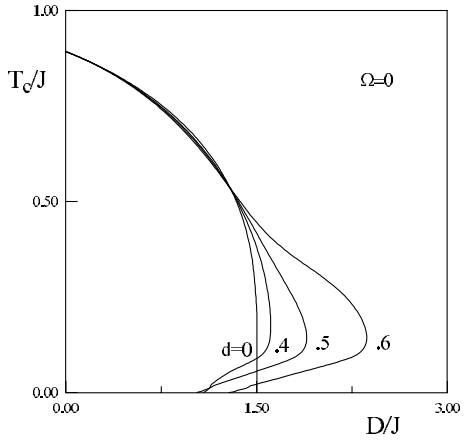

(a)

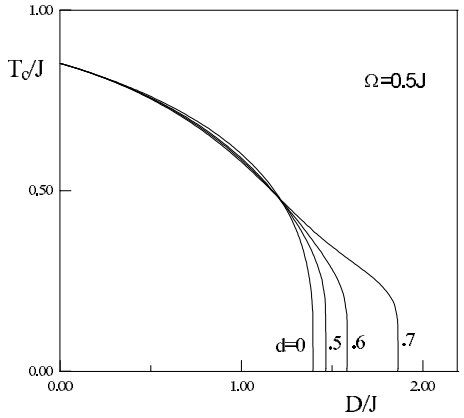

(b)

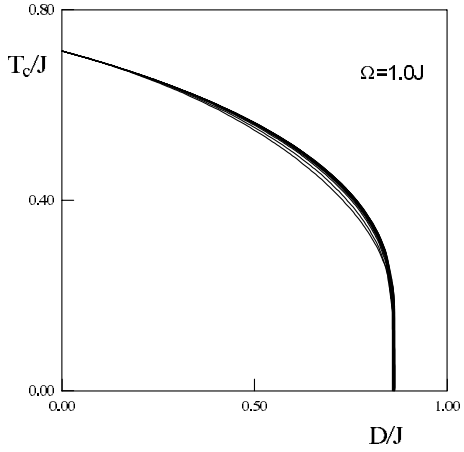

(c)

Fig. 2. The phase diagram in $T-D$ plane of the mixed spin-1/2 and spin-1 transverse Ising model on the honeycomb lattice ($N = 3$) is shown for different values of d when Ω is kept fixed: ($\Omega = 0$ (a), $\Omega = 0.5$ J (b), $\Omega = 1.0$ J (c)).

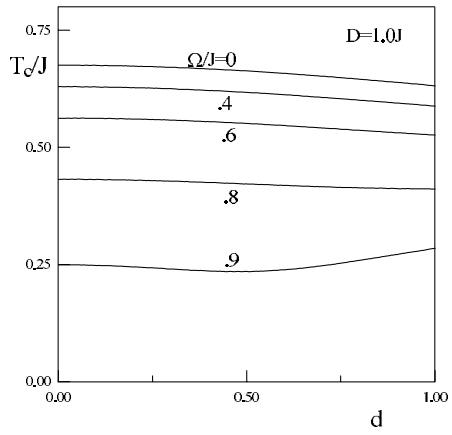

(a)

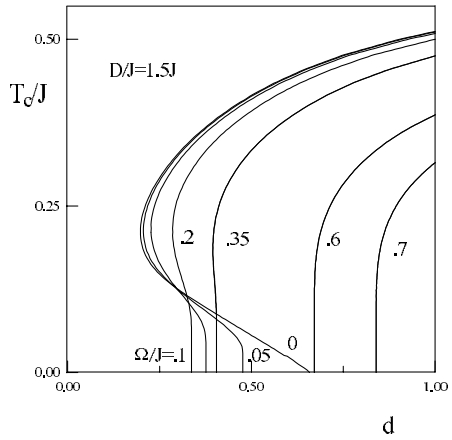

(b)

Fig. 3. The variation of the transition temperature with d for the honeycomb lattice ($N = 3$), when the mean value of the crystal field is kept fixed ($D = 1$ J (a) and $D = 1.5$ J (b)). The number accompanying each curve denotes the value of Ω/J.

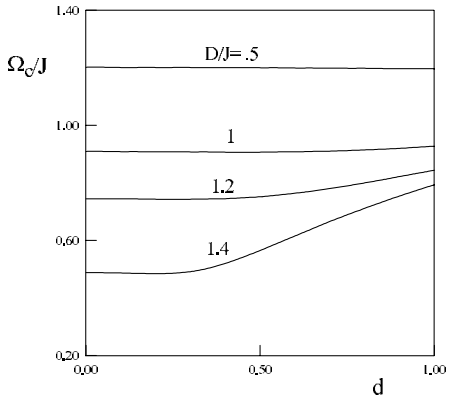

Fig. 4. Plot of the critical value Ω_c of the transverse field as a function of d for the honeycomb lattice ($N = 3$). The number accompanying each curve denotes the value of D/J.

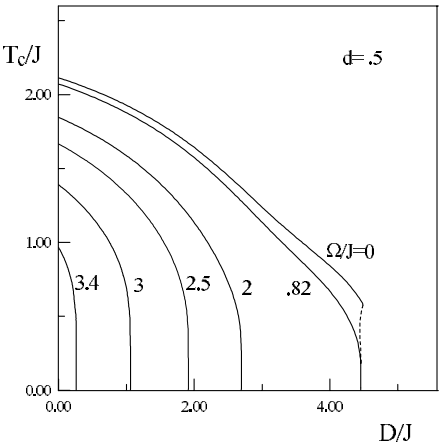

Fig. 5. The phase diagram in $T-D$ plane of the mixed spin-1/2 and spin-1 transverse Ising model on the simple cubic lattice ($N = 6$), when $d = 0.5$. The number accompanying each curve denotes the value of Ω/J. Dashed line corresponds to the tricritical line.

phenomenon) gradually decreases with the increase of Ω and disappears for Ω larger than $\Omega = 0.48$ J.

On the other hand, it is interesting to study, at the ground state of the system, the effects of the fluctuation of the crystal field on the critical value Ω_c of the transverse field. For a given mean value D of the crystal field, the changes of Ω_c with d is obtained from the solution of the equation (57) keeping $T_c = 0$. This is plotted in Figure 4, for several values of D. The results for the critical transverse field Ω_c look rather independent of d when D is less than $D = 0.96$ J. For larger values of D, Ω_c increases slightly with increasing values of d; but when D approaches its critical value $D_c = 1.5$ J, Ω_c curve expresses rapid increase with d.

3.2 The simple cubic lattice

First, we have to point out for the simple cubic lattice ($N = 6$), when ignoring the fluctuation of the crystal field ($d = 0$) [28], that the transition is of first order for small Ω and D near its critical value $D_c = 3$ J; the remaining part of the transition surface is always of second order for any values of the transverse and crystal fields. Now, by means of equations (57, 59), we are in a position to examine the effects of crystal field disorder on the phase diagram of the corresponding pure case ($d = 0$).

Figure 5 shows the phase diagram in $T-D$ plane for a fixed value of $d\,(d = 0.5)$ and various values of Ω. In the absence of the transverse field (Ω/J $= 0$), and in contrast to the case $N = 3$ (Fig. 1), the critical line ends in a tricritical point. As seen in the figure, this tricritical behaviour is kept by the system when the strength of the transverse field Ω is less than 0.82 J. If Ω belongs to the range 0.82 J $< \Omega < \Omega_c$ ($\Omega_c = 3.516$ J being the critical value of the transverse field), the tricritical behaviour disappears and

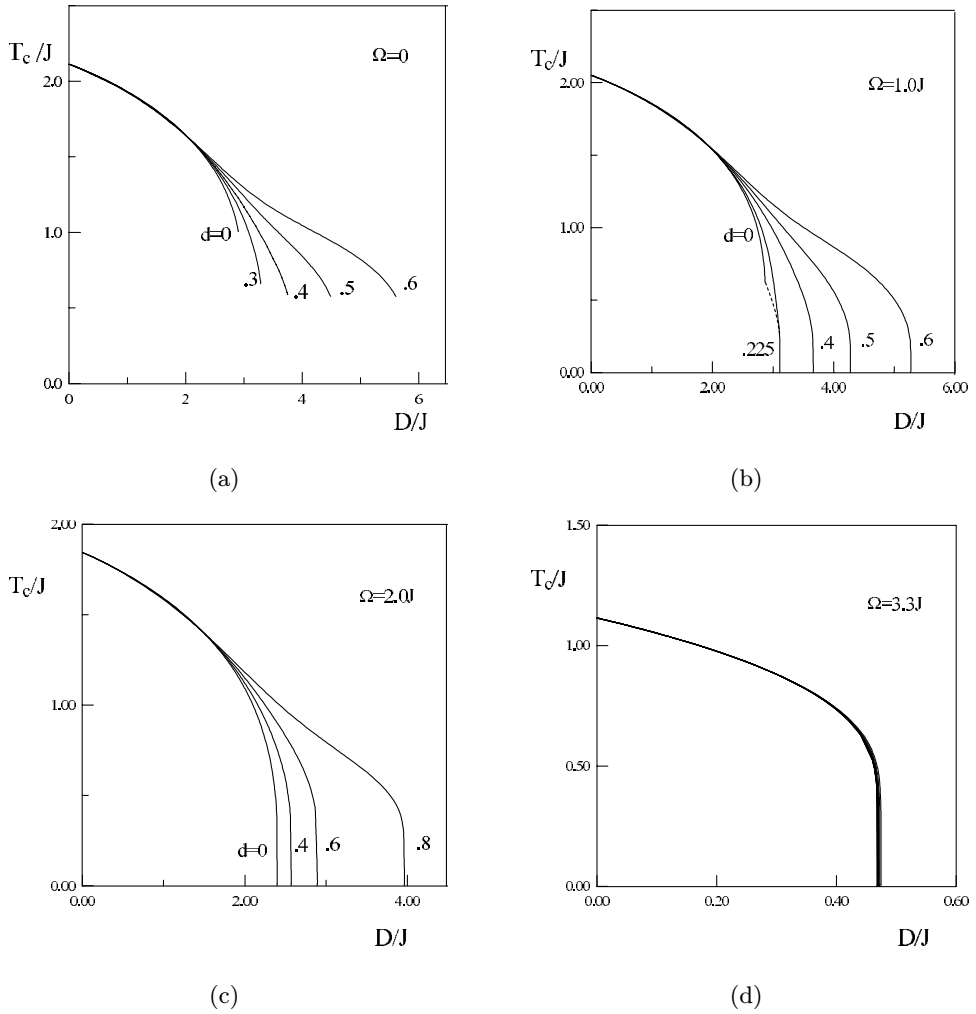

Fig. 6. The phase diagram in $T-D$ plane of the mixed spin-1/2 and spin-1 transverse Ising model on the simple cubic lattice ($N = 6$) is shown for different values of d when Ω is kept fixed: $\Omega = 0$ (a), $\Omega = 1.0$ J (b), $\Omega = 2.0$ J (c), $\Omega = 3.3$ J (d).

all transitions are of second order for any mean value D of the crystal field interaction.

In Figure 6a, the critical temperature is plotted as a function of D in zero transverse field ($\Omega = 0$) and various values of d. For $d = 0$, the critical temperature decreases with the increase of D and ends in a tricritical point. As shown in the figure, the system keeps this tricritical behaviour even when d takes a finite value. Such qualitative behaviour of the phase diagram is exhibited by the system when the transverse field strength belongs to the range $0 \leq \Omega/\mathrm{J} < 0.807$. In the region $0.807 < \Omega/\mathrm{J} < 1.165$, the T_c curves which correspond to high fluctuations of the crystal field (high values of d) become second order for any D; while the tricritical behaviour exists only for small d as is shown in Figure 6b for $\Omega = 1.0$ J. If $1.165 \leq \Omega/\mathrm{J} < 3.24$, we obtain a phase diagram with no tricritical behaviour for any d as is plotted in Figure 6c for $\Omega = 2.0$ J. We note that in these three ranges of Ω when D is small, T_c does not depend on d and, due to the fluctuation of the crystal field, the ferromagnetic frontier lines can take a finite value D larger than its critical value $D_c = 3$ J. Here again, when Ω approaches ($3.24\,\mathrm{J} < \Omega < \Omega_c$) to its critical value $\Omega_c = 3.516$ J, the transition temperature, as a function of the mean value D, becomes independent of the fluctuation of the crystal field as shown in Figure 6d for $\Omega = 3.3$ J. These two latter properties of the system with $N = 6$, are similar to those (Fig. 2b and c) obtained for the honeycomb lattice.

Now, we investigate more precisely the effects of d on T_c with various values of the transverse field strength. For low values of D, we obtain (for instance Fig. 7a, for $D = 1.0$ J) a very small variation of T_c with d like in the case $N = 3$ (see Fig. 3a). But for relatively high values of D, the model on the simple cubic lattice behaves differently from the case $N = 3$. In fact, as is seen in Figure 7b with $D = 3$ J, a tricritical behaviour appears in the phase diagram for low values of the transverse field Ω and completely disappears for larger values of Ω (but less than Ω_c).

At the ground state of the system, the variation of the critical value Ω_c of the transverse field with d is plotted in

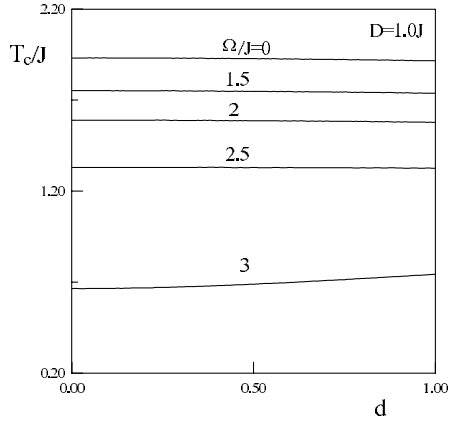

(a)

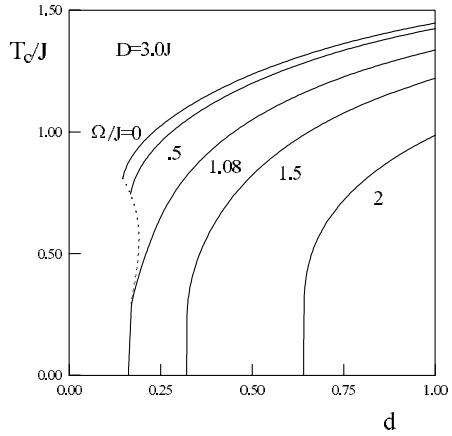

(b)

Fig. 7. The variation of the transition temperature with d for the simple cubic lattice ($N = 6$), when the mean value of the crystal field is kept fixed ($D = 1$ J (a) and $D = 3$ J (b)). The number accompanying each curve denotes the value of Ω/J. Dashed line corresponds to the tricritical line.

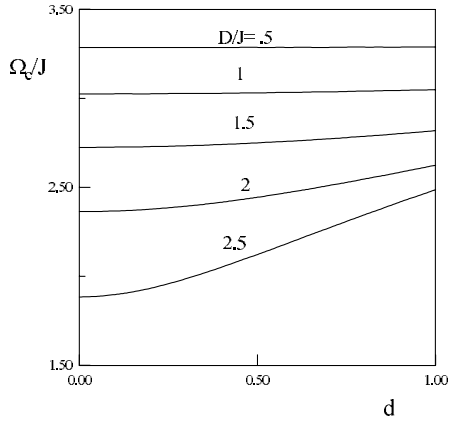

Fig. 8. Plot of the critical value Ω_c of the transverse field as a function of d for the simple cubic lattice ($N = 6$). The number accompanying each curve denotes the value of D/J.

Figure 8 for different values of D. The obtained phase diagram is qualitatively similar to that obtained in the case of the honeycomb lattice. We note that for the simple cubic lattice, the different behaviour (independence and variation of Ω_c with d) expressed in the figure, are obtained when the mean value of the crystal field is less than or greater than 0.76 J, respectively.

This work was supported by the agreement of cooperation between the CNR (Morocco) and the DFG (Germany). We want to thank the both organizations. One of us (N.B) acknowledges the hospitality of the Institut für Theoretische Physik der Universität zu Köln.

References

1. P.-G. de Gennes, Solid State Commum. **1**, 132 (1963).
2. R. Blinc, B. Zeks, *Soft Modes in Ferroelectrics and Antiferroelectrics* (North-Holland, Amsterdam, 1974).
3. R.J. Elliott, G.A. Gekring, A.P. Malozemoff, S.R.P. Smith, N.S. Staude, R.N. Tyte, J. Phys. C **4**, 179 (1971).
4. Y.L. Wang, B. Cooper, Phys. Rev. **172**, 539 (1968).
5. R.B. Stinchcombe, J. Phys. C **6**, 2459 (1973).
6. P. Pfeuty, Ann. Phys. (N.Y) **57**, 79 (1970).
7. R.J. Elliott, I.D. Saville, J. Phys. C **7**, 3145 (1974).
8. A.B. Harris, J. Phys. C **7**, 3082 (1974).
9. R.B. Stinchcombe, J. Phys. C **14**, L263 (1981).
10. F.C.Sà. Barreto, I.P. Fittipaldi, B. Zeks, Ferroelectrics **39**, 1103 (1981).
11. F.C.Sà. Barreto, I.P. Fittipaldi, Physica A **129**, 360 (1985).
12. Chuan-Zhang Yang, Jia-Lin Zhong, Phys. Stat. Sol. (b) **153**, 323 (1989).
13. Jia-Lin Zhong, Jia-Lin Li, Chuan-Zhang Yang, Phys. Stat. Sol. (b) **160**, 329 (1990).
14. M. Saber, J.W. Tucker, J. Magn. Magn. Mater. **102**, 287 (1991).
15. A. Benyoussef, H. Ez-Zahraouy, Phys. Stat. Sol. (b) **180**, 503 (1993).
16. L. Néel, Ann. Phys. Fr. **3**, 137 (1948).
17. M. Drillon, E. Coronado, D. Beltran, R. Georges, J. Chem. Phys **79**, 449 (1983).
18. S.L. Schofield, R.G. Bowers, J. Phys. A **13**, 3697 (1980).
19. N. Benayad, Z. Phys. B **81**, 99 (1990).
20. B.Y. Yousif, R.G. Bowers, J. Phys. A **17**, 3389 (1984).
21. Kun-Fa Tang, J. Phys. A **21**, L1097 (1988).
22. N. Benayad, A. Klümper, J. Zittartz, A. Benyoussef, Z. Phys. B **77**, 333 (1989).
23. G.M. Zhang, C.Z. Yang, Phys. Rev. B **48**, 9452 (1993).
24. T. Kaneyoshi, J. Phys. Soc. Jpn **56**, 2675 (1987).
25. N. Benayad, A. Klümper, J. Zittartz, A. Benyoussef, Z. Phys. B **77**, 339 (1989).
26. C. Domb, Adv. Phys. **9**, 149 (1960).
27. L.L. Conçalves, Phys. Scripta **32**, 248 (1985).
28. N. Benayad, R. Zerhouni, Phys. Stat. Sol. (b) **201**, 491 (1997).
29. N. Boccara, Phys. Lett. A **94**, 185 (1983).
30. A. Benyoussef, N. Boccara, J. Phys. **44**, 1143 (1983).
31. H. Ez-Zahraouy, M. Saber, J.W. Tucker, J. Magn. Magn. Mater. **118**, 129 (1993).
32. P. Tomczak, E.F. Sarmento, A.F. Siqueira, A.R. Ferchmin, Phys. Stat. Sol. (b) **142**, 551 (1987).